Optimal Energy Management of A Power Transmission Grid under A Heatwave Exposure

Ali Alawad[§], Ahmad Alnakhli*, Payman Dehghanian[±]
Department of Electrical and Computer Engineering
The George Washington University
800 22nd St NW, Washington, Suite 5900, DC 20052, USA.
{alawad[§],*alnakhli,[±]payman}@gwu.edu

***Abstract*— The recent increase in number of weather events across the globe has grabbed the attention of researchers and industry. Weather related events such as extreme temperatures, hurricanes and earthquake are responsible of the majority of power outages in the last decade. In particular, extreme temperatures can affect the power network in three levels: generation, transmission and distribution. For instance, during a heatwave the efficiency and output of power plants will decrease, and the transmission lines will operate at their limits. This happens while the demands in the distribution side will increase above the usual peak. Planning for such events require careful operation and planning of the entire system. In this paper, an optimal operation strategy is proposed for transmission systems under the heatwave exposure taking into consideration the impacts of hourly temperature on load profiles and available capacity and efficiency of renewable and non-renewable power generations, transmission lines capacity, and load curtailment. The proposed approach has been applied to capture the impacts of the heatwave event occurred in the state of Texas in August 2011. The results demonstrate the effectiveness of the proposed operation strategy in quantifying the impact of heatwaves on the transmission network operation.**

***Index Terms*—heatwave; capacity; efficiency; operation cost; power transmission system; thermal power units; PV energy; wind; ambient temperature.**

NOMENCLATURE

A. Sets

$g \in \mathbf{G}$	Set of all generating units
$i,j \in \mathbf{B}$	Set of all transmission busses.
$d \in \mathbf{D}$	Set of load points.
$z \in \mathbf{Z}$	Set of temperature clustering zones.
$k \in \mathbf{K}$	Set of transmission lines.
$t \in \mathbf{T}$	Set of operation time steps.
$pv \in \mathbf{PV}$	Set of all solar PV units.
$w \in \mathbf{W}$	Set of all wind turbines.
$\boldsymbol{K_i, K_s, K_r}$	Set of transmission lines connected to bus *i*, set of transmission lines with the sending end bus *i* and set of transmission lines with receiving end bus *j*.

B. Parameters and Constants

$C_{i,t}^{G}$	Price of power generated from the power plant *g* connected to bus *i* at time *t* ($/MW).
$C_{g,t}^{fix}$	The fixed (no-load) cost of generating unit *g* at time *t*.
$VOLL_i$	Value of lost load connected to bus *i*.
γ_i	PV power temperature coefficient ($^oC^{-1}$) connected to bus *i*.
NG	Number of generator units.
NL	Number of load points.
NT	Number of operation time steps.
$P_i^{G,max}, Q_i^{G,max}$	Maximum active and reactive power capacity of generating unit *g* connected to bus *i*.
$P_{i,t}^{Load}, Q_{i,t}^{Load}$	Active and reactive power demand for the load connected to bus *i* at time *t*.
$P_k^{Line,max}$	Maximum power flow limit of line *k* (MW); also known as line rating or line ampacity,
$P_{i,t}^{PV,heat}$	Output power of PV panel connected to bus *i* during the heat wave at time *t* (MW).
$P_i^{PV,STC}$	Power provided by PV panel connected to bus *i* under standard test condition (STC) (MW).
$P_{i,t}^{W,max}$	Maximum power output of wind turbine *w* connected to bus *i* at time *t* (MW).
$T_{z,t}^{a}$	Ambient temperature in zone *z* at time *t* (^oC).
$G_{z,t}$	Incident solar irradiance in zone *z* at time *t* (W//m^2).
$\Delta P_{i,t}^{G}$	Power correction factor for generating unit *g* connected to bus *i* at time *t*, due to ambient temperature $T_{z,t}^{a}$ (%)$I_{b,t}$.
$I_{k,t}$	Capacity correction factor for line *k* due to ambient temperature $T_{z,t}^{a}$ (%).
Y_G, Y_K, Y_{K0}	Conductance, series admittance and shunt admittance of transmission line *k*, respectively.
G_{STC}	Solar irradiance at STC (W/m^2).
$H_{g,i}$	The nominal heat rate of generator *g* at bus *i*.
B_g	The fuel price of generating unit *g*.
A_w	Area swept by the rotor of wind turbine *w*.
ρ_a	Air density (kg/m^3).
$v_{i,z,t}$	Wind speed for wind turbine connected to bus *i* in zone *z* at time *t* (m/s).
$\varepsilon, \sigma, D_k, a_s$	Emissivity of the conductor surface, the Stefan-Boltzmann constant, Diameter of the conductor, and Absorptivity of the conductor surface, respectively.
ζ^W, C^P	Wind turbine efficiency (%) and the Albert Betz constant, respectively.

C. Decision Variables

$P_{i,t}^{G}$	Active power provided by generating unit *g* connected to bus *i* at time *t* (MW).

2021 North American Power Symposium (NAPS) | 978-1-6654-2081-5/21/$31.00 ©2021 IEEE | DOI: 10.1109/NAPS52732.2021.9654592

$P_{i,t}^{W}$	Power output of wind turbine *w* connected to bus *i* at time *t* (MW).
$T_{i,t}^{PV}$	The PV cell temperature connected to bus *i* at time *t* (^{o}C).
$\boldsymbol{P_{k,t}^{Line}}, \boldsymbol{Q_{k,t}^{Line}}$	Active and reactive power flow through line *k* at time *t*.
$\boldsymbol{P_{i,t}^{Shd}}, \boldsymbol{Q_{i,t}^{Shd}}$	Active and reactive load curtailment in bus *i* at time *t*.
$u_{i,t}^{g}$	Binary variable that specifies the on/off status of generating unit *g* connected to bus *i* at time *t* (1: on, 0: off).
$u_{i,t}^{Shd}$	Binary variable that specifies the curtailment status of load *d* connected to bus *i* at time *t* (1: being curtailed, 0: no curtailment).
$\theta_{k,t}$	Voltage phase angle difference across both ends of the transmission line *k* at time *t*.
$\Delta V_{i(j),t}$	Bus voltage magnitude deviation at bus *i* or *j* at time *t*.
$V_{i(j),t}$	Bus voltage magnitude at bus *i* or *j* at time *t*.

I. Introduction

It has been evidenced since the 20th century started that the average annual temperatures across the United States have increased approximately $0.8^{o}C$, within 2001 to 2010 being the warmest decade recorded in the history [1]. Global warming not only causes the average temperature to rise, but also leads to more frequent and severe extreme weather events such as heat waves [1]. Looking again at some figures for the U.S. alone, we observe that the estimated average annual cost of power outages caused by severe weather events (including hot and cold waves, as well as hurricanes, floods, etc.) ranged between U.S. $18 and 33 billion between 2003 and 2012 [2].

Over the past few years, many research efforts have been conducted to study the impacts of climate change on electric power grids from different aspects. In [3, 4], high ambient air and water temperatures reduce both the efficiency and available generating capacity of thermal power plants. Capacity deratings also occur because the higher ambient air temperatures lead to lower mass density of intake air, resulting in less fuel mass that can be ignited, and therefore reduced power output. Similar effects apply to natural gas combustion turbines and natural gas combined cycle plants [5], [6]. Response functions are generally linear, in the form of a constant decrease in power output per degree change above a reference temperature. For example, one study conducted by the California Energy Commission (CEC) found that natural gas combined cycle power plant capacity decreases by 0.3-0.5 percent for each $1^{o}C$ increase above a reference temperature of $15^{o}C$ [7]. Similar studies examining the temperature response of nuclear power plant output have found a decrease of approximately 0.1-0.5 percent for every $1^{o}C$ increase in ambient air temperature [8].

Operating temperature also decreases both the electrical efficiency and the power output of a solar photovoltaic (PV) module. However, the operating temperature of the solar cell depends on a range of factors, including the ambient air temperature, wind speed, solar radiation flux/irradiance, and material and system-dependent properties. While establishing a direct relationship between solar PV performance and ambient temperature and other weather variables is challenging, solar PV temperature response functions have been reviewed and presented in the literature [9]. High water temperatures can also cause threshold impacts. For example, power plants may be forced to curtail operations fully or partially when the intake cooling water exceeds the operating design temperatures [10].

High temperatures also increase the power transmission and distribution line losses and reduce the carrying capacity. Average electricity transmission and distribution losses are about 5% in the United States [11]. The resistance of power lines increases with temperature, leading to greater resistive loss [12]; however, the impact of ambient temperature on resistive losses is generally considered to be negligible compared to impacts on total carrying capacity [13]. The line capacity is limited by the maximum normal operating temperature, typically $80^{o}C$. The operating temperature of the power line depends on several factors, including the ambient temperature, current flowing through the line, and wind speed, which affects the ability of the line to get rid of the excess heat, and is generally much higher than the ambient temperature.

As previously explained, higher temperatures during heat waves affect the entire system generation, transmission, and load demand behavior. Without modeling and capturing such effects on different power grid components, one cannot evaluate the overall impacts of the heat waves on the power grid operation. This paper describes an operation cost model within an energy management system to quantify the impacts of heat waves on power grid operation considering different thermal power stations and transmission lines. The main technical challenge of considering the derating effects in the system due to heatwaves stems from the fact that the output capacity and net efficiency of different power units will be diverse as they will be exposed to different temperature zones on an hourly basis. In this paper, hourly derating impacts is reflected into a proposed mixed integer linear programming (MILP) mode for power transmission operation when exposed to heatwaves.

II. Problem Formulation

In this section, the mathematical models for thermal power plants, PV, wind turbines, and transmission lines are addressed to consider the impact of excess temperatures on their operational constraints. Whenever applicable, the impact of temperature on the component capacity and net efficiency has been modeled. For more accuracy, temperature clustering is conducted for the state of Texas to be able to divide the networks' generating units into zones, each will be exposed to different temperature during the considered heatwave duration. Here, each time step of the analysis is assumed to be one hour, which means the power levels (in MW) would be equivalent in value to the energy levels (in MWh). In the absence of this assumption, all power values would have to be multiplied by the duration of the time step in order to derive the energy levels.

A. Electrical Transmission System Clustering Based on Historical Summer Temperature Data

To identify homogeneous regions in the state of Texas in terms of summer extreme temperatures, we use the *k*-means clustering algorithm originating from multivariate extreme value theory [14]. This technique is suitable to extract the spatial dependencies from series of seasonal maxima. Note that no geographical information is used to cluster the stations. Instead, we use a statistical distance to measure the proximity of two stations with respect to their maxima.

The clustering algorithm is applied to the NOAA observations over the summer period (May-September) with daily maximum and average temperatures (2000–2020). The algorithm identifies different geographical regions (see Fig. 1). In the proposed model, we chose four cities in the state of Texas that had different temperature zones.

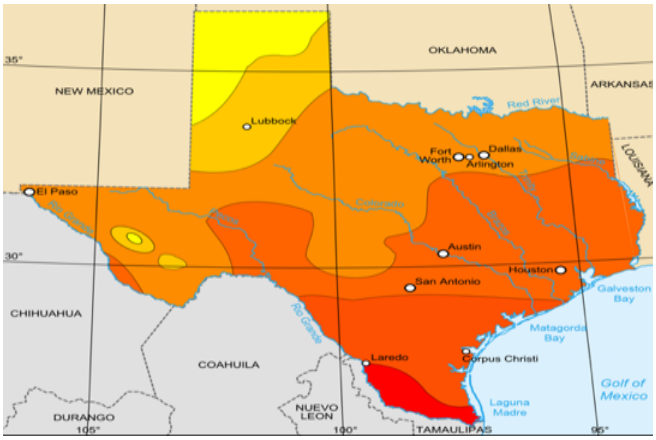

Fig. 1. Summer temperature's clustering zones in the state of Texas.

B. Characterization of Temperature Impacts on Thermal Power Generation

This section will first characterize the performance of some thermal power generation units such gas-fired plants and nuclear plants as functions of ambient temperature. Natural gas combustion turbines (NGCT) and natural gas combined cycle (NGCC) have been chosen here because they are the most used gas-fired plants in the U.S. [15].

1) Generation Capacity Derating

It should be noted that the output power capacity of the generator will be limited by its maximum allowable power $P_i^{G,max}$. As mentioned before, $P_i^{G,max}$ varies with temperature; therefore, a modified maximum power based on the ambient temperature should be used instead. To do so, we have used the data available in [16] and have fit a linear curve to as indicated in Fig. 2. It should be noted that this particular gas turbines unit has been chosen for demonstration purposes, while different generating units may demonstrate slightly different behavior with temperature variations.

$$\Delta P_{i,t}^{G} = -0.6 \cdot T_{z,t}^{a} + 109 \qquad (1)$$

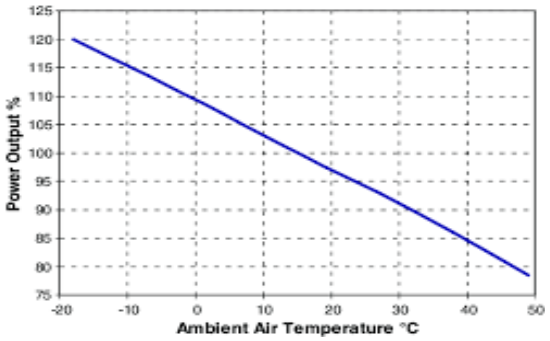

Fig. 2. Variation of power output with ambient air temperature for a given gas turbine [11].

2) Generation Efficiency Derating

Heat rate is a term commonly used in power systems to indicate the power plant efficiency. It is defined as the amount of energy used by a generator to produce one unit of electricity output. The heat rate is an inverse function of efficiency; that is a lower heat rate is more desired. However, the density of input air decreases with increasing ambient temperature, resulting in more fuel needed to compress the same amount of air mass. The increased fuel consumption per unit energy output leads to increased heat rate and decreased net efficiency of a NGCT/NGCC units. The normalized heat rate can be expressed as a function of ambient temperature. Using such derating functions combined with hourly temperature data, we can adjust the fuel efficiency on an hourly basis in the production cost formula as follows [18]:

$$C_{i,t}^{G} = C_{g,t}^{fix} u_{i,t}^{g} + B_g \sum_{g=1}^{NG} P_{i,t}^{G} \Delta T \frac{H_{g,i}}{\Delta P_{i,t}^{G}} \qquad (2)$$

C. Renewable Units

1) Wind Energy

The output power of wind energy conversion system can be found as a function of the wind speed and the swept area of the turbine rotor, among other parameters as described in [18]:

$$P_{i,t}^{W} = o.5\, \zeta^{W}\, C^{P}\, \rho^{a}\, A_w v_{i,z,t}^{3} \qquad (3)$$

The following parameters have been used for wind turbine as follows: ζ^W= 40%, C^P= 0.593, ρ^a= 1.225 kg/m3, A_w = 353 m^2 and cut-in and cut-out wind speed: 2.7 m/s and 25 m/s according to [18].

2) Solar Energy

The PV generator has been modeled by a linear power source according to the ambient temperature and the irradiance level is obtained from [19], where parameters are obtained from the information available in the manufacturer data sheets [nominal operating cell temperature (NOCT) and standard test condition (STC)]:

$$P_{i,t}^{PV,heat} = [P_i^{PV,STC} \times \frac{G_{i,z,t}}{G_{STC}} \times [1 - \gamma_i \times (T_{i,t}^{PV} - 25)]] \qquad (4)$$

$$T_{i,t}^{PV} = T_{z,t}^{a} + \frac{G_{i,z,t}}{800} \times (NOCT - 20) \qquad (5)$$

where $P_i^{PV,STC}$ is assumed to be 200W, G_{STC} = 1000 W/m^2, γ = 0.043% and the cell temperature $T_{i,t}^{PV}$ is obtained from (5). NOCT = 45.5^oC according to [19].

D. Transmision Line Capacity

In expanded form, the rated ampacity of an overhead conductor can be expressed in terms of ambient weather conditions (temperature and wind speed), solar insolation, and cable properties (diameter, surface area and material properties). Following the IEEE Standard 738-2006, the formula to calculate the reduction in the ampacity of the transmission lines with temperature increase will be applied in this paper.

$$I_{k,t} = \sqrt{\frac{\pi \cdot H_{k,i} \cdot D_k \cdot (T_{k,t} - T_{z,t}^a) + \pi \cdot \varepsilon \cdot \sigma \cdot D_k \cdot (T_{k,t}^4 - T_{z,t}^{a\,4}) - G_{z,t} \cdot D_k \cdot \alpha_s}{R(T_{k,t})}} \quad (6)$$

E. Emergency Operation Mode

Inspired by [20], constraint (7) shows the load curtailment cost in the emergency operation mode, which is penalized with the value of lost load (VOLL) and is here considered \$800/MWh. Finally, constraints (8) enforce the limits for load curtailments:

$$C_{i,t}^{Shd} = P_{i,t}^{Shd} \cdot VOLL_i \quad (7)$$

$$0 \leq P_{i,t}^{Shd} \leq P_{i,t}^{Load} \quad (8)$$

F. The Objective Function

The objective function is to minimize the total operational cost of the network, while ensuring that the balance between available generation and load demand is maintained. It should be emphasized that our focus is on the real-time cost of system operation, and we do not consider other expenses such as maintenance and capacity expansion. The problem is formulated while considering the impact of ambient temperature during heat waves on the available capacity and efficiency of various system components. It is assumed that the operational costs incur due to the usage of any generator and loads shedding except for non-dispatchable units that operate in the maximum power point tracking (MPPT) mode. Renewable units are therefore not incorporated into the cost function; however, they are considered in the generation-load balance equation. The objective function is therefore defined as follows:

$$min\{\sum_{t=1}^{NT}\{\sum_{g=1}^{NG} C_{i,t}^G . u_{i,t}^g + \sum_{i=1}^{NL} C_{i,t}^{Shd} . u_{i,t}^{Shd}\}\} \quad (9)$$

The first term of the objective function indicates the cost of the power generation, while the second terms represent the costs associated with load curtailments. The objective function in (9) would be solved subject to the following constraints:

$$|P_{k,t}^{line}| \leq P_k^{line,max} . I_{b,t} \quad , b \in \mathbf{B} \quad (10)$$

$$0 \leq P_{i,t}^G \leq P_i^{G,max} . \Delta P_{i,t}^G \quad , i \in \mathbf{G} \quad (11)$$

$$0 \leq P_{i,t}^W \leq P_{i,t}^{W,max} \quad , i \in \mathbf{W} \quad (12)$$

$$0 \leq P_{i,t}^{PV} \leq P_{i,t}^{PV,heat} \quad , i \in \mathbf{PV} \quad (13)$$

$$0 \leq P_{i,t}^{Shd} \leq P_{i,t}^{Load} \quad , i \in \mathbf{D} \quad (14)$$

G. Power Balance Constraints

The real and reactive power should be balanced between generation and load at all times, as shown in constraints (15) and (16). Inspired by [21], we utilized a linearized AC power flow model to obtain the real and reactive power flow of the transmission lines, as reflected in constraints (17) and (18).

$$\sum_{g\in G} P_{i,t}^G + \sum_{pv\in PV} P_{i,t}^{PV} + \sum_{w\in W} P_{i,t}^W + \sum_{k\in K_r}(P_{k,t}^{line}) + \sum_{shd\in D} P_{i,t}^{Shd} = \sum_{k\in K_s}(P_{k,t}^{line}) + \sum_{d\in D} P_{i,t}^{Load} \quad (15)$$

$$\sum_{g\in G} Q_{i,t}^G + \sum_{pv\in PV} Q_{i,t}^{PV} + \sum_{w\in W} Q_{i,t}^W + \sum_{k\in K_r}(Q_{k,t}^{line}) + \sum_{shd\in D} Q_{i,t}^{Shd} = \sum_{k\in K_s}(Q_{k,t}^{line}) + \sum_{d\in D} Q_{i,t}^{Load} \quad (16)$$

$$P_{k,t}^{line} = (\Delta V_{i,t} - \Delta V_{j,t})\, Y_G - Y_K \cdot \theta_{k,t} \quad (17)$$

$$Q_{k,t}^{line} = -(1 + 2\Delta V_{i,t})\, Y_{K0} - (\Delta V_{i,t} - \Delta V_{j,t}) Y_K - Y_G \cdot \theta_{k,t} \quad (18)$$

III. Numerical Results and Discussions

A. Test System Description

To evaluate the performance of the proposed model, a modified IEEE 118-bus test system is employed as a case study. As shown in Fig. 3, the test system includes 15 thermal power units, 2 wind farms, 4 solar farms, 118 buses, and 186 transmission lines. The maximum load demand is assumed 6000 MW. The characteristics and data on system generators, buses and transmission lines are taken from [22]. We assumed there are two wind farms with the capacity of 550 MW, and four solar farms with capacity of 1500 MW. The PV and wind energy represent 18% of the total energy production.

The case studies presented here are related to the period of a notable heatwave event on August 3–5, 2011 in the state of Texas. After temperature clustering, 4 cities have been chosen (San Antonio, Austin, Dallas and Lubbock) which are represented in Fig. 3. The load profile has been adjusted to simulate the load behavior during the heatwave [18]. The total period of the study is considered 72 hours over the three days of the heatwave event. In our simulations, the actual ambient temperatures, wind speed and solar irradiance data have been used for the time-period and across the geographical locations.

Two case studies were carried to find the objective function in (9) subject to the constraints (1)-(18). The first case study represents the network operation without temperature effect while the second one considers temperature effects. To determine the dispatch without the effect of temperature, ambient temperature has been set at 25 ^oC. This value provides the nominal ratings for all components in the network. The optimization problem is been solved using Cplex solver in AMPL. All simulations have been done on a Laptop with an Intel Core i7 processor and 16 GB of memory.

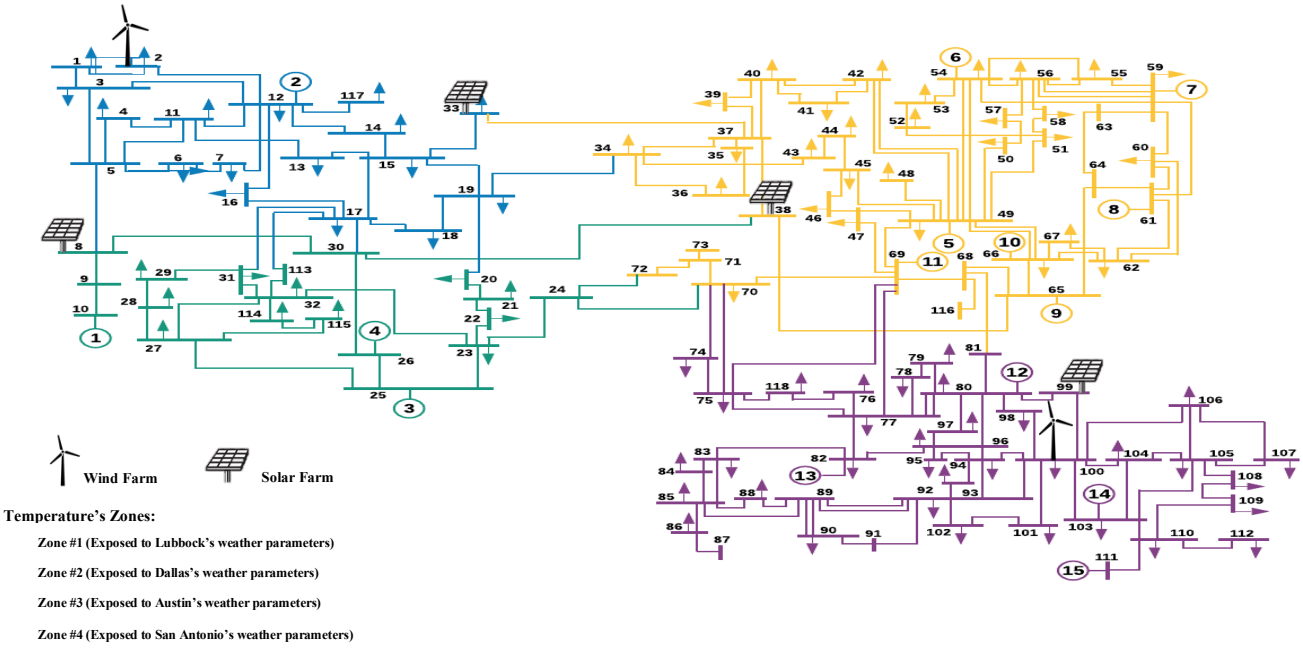

Fig. 3. The modified IEEE 118-bus test system.

TABLE I. LOCATIONS AND CHARACTERISTICS OF POWER GENERATORS

Generation Type	Bus No.	$P_i^{G,max}$ (MW)	Fuel Cost ($/fuel unit)	Power Correction Factor $\Delta P_{i,t}^{G}$(%)
Nuclear plant	10	550	0.217	$\Delta P_{i,t}^{G} = -0.48 \cdot T_{z,t}^{a} + 112$
Natural gas-NGCC	12	185	1.052	$\Delta P_{i,t}^{G} = -0.52 \cdot T_{z,t}^{a} + 113$
	25	320	0.434	
	26	414	0.308	
	49	304	0.467	
	54	255	1.724	
	59	255	0.606	
	61	260	0.588	
	65	491	0.2493	
	66	492	0.2487	
Natural gas-NGCT	69	805.2	0.1897	$\Delta P_{i,t}^{G} = -0.2 \cdot T_{z,t}^{a} + 102.5$
	80	577	0.205	
	82	452	0.381	
	103	244	2	
	111	255	2.173	
Wind Farms	2	275	0	N/A
	100	275	0	
PV Farms	8	435	0	Constraints (4), (5)
	33	450	0	
	38	245	0	
	99	370	0	

B. *Results and Discussions*

Figure 4 shows the total power that comes from all generation units (thermal, PV and wind) with and without temperature consideration. When the temperature effects are not considered, the generation power capacity and efficiency will be at the maximum level for most of the time. However, considering temperature effect resulted in a decrease in the total generation output as the temperature increases and that will clear during hours 9–20, 33–45 and 57–69 (which is corresponding to 9 am to 8 pm per day) when the temperature exceeds $35^{o}C$.

Figure 5 illustrates the total thermal power injected into the grid with and without heatwave effect. The total power from these units is reduced within a range of (2-10%) whenever temperature is higher than $40^{o}C$, and the reduction percentage will depend on the types of the thermal plant (gas, nuclear, coal) and outdoor temperature. This can be attributed in part to the reduction in plant maximum capacity and efficiency as shown in constraints (1), (2).

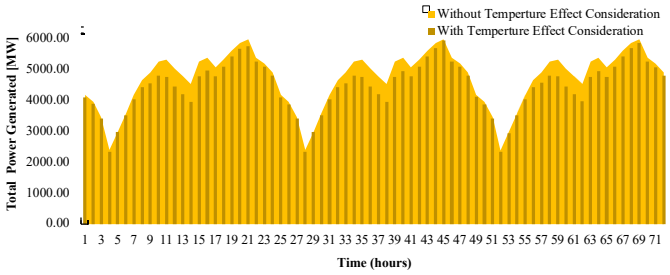

Fig. 4. Total power generation with and without temperature effects.

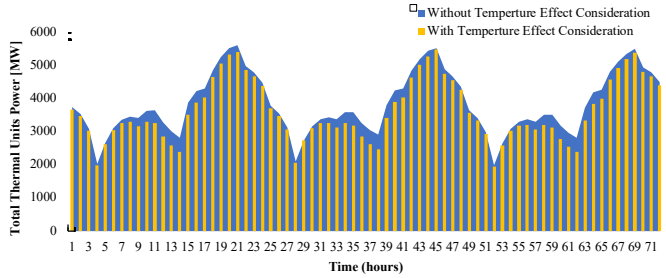

Fig. 5. Total thermal generating units power output with and without temperature effect.

Figure 6 illustrates the total PV and wind power production output with and without temperature consideration over a 3-day time-period. The total PV output differs by about 7% when actual outdoor air temperatures are evaluated, while the wind power shows no dependency on ambient temperatures as shown in constraint (3).

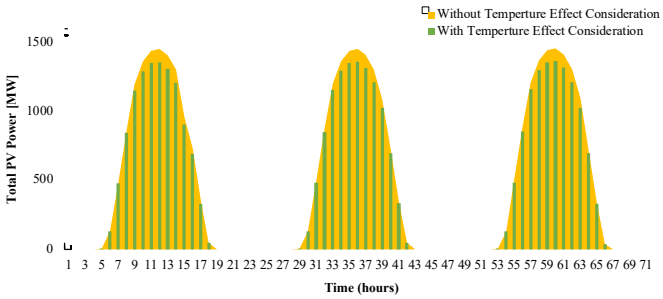

Fig. 6. Total PV power output with and without temperature effect.

Finally, Fig. 7 shows the amount of load demand curtailed during the heatwave event. We can notice that a considerable amount of load demand will be curtailed in the first day period as the highest temperature was recorded in the first day.

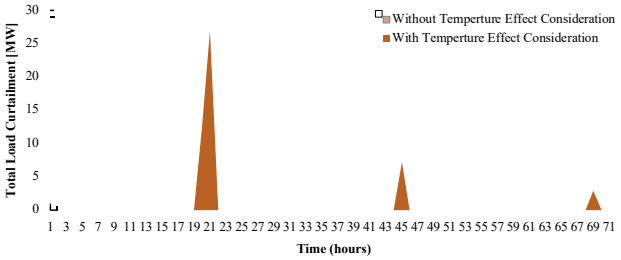

Fig. 7. Total curtailed power with and without temperature effect.

The total operational cost comparison between the two case studies is summarized in the following table:

TABLE II. COST COMPARISON BETWEEN THE STUDIED CASES

Cost ($)	Case I	Case II
Thermal power generation	92474.7	101557
Load demand power curtailed	0	2002.65
Renewable power (PV&Wind)	0	0
Total cost	92474.7	103560

IV. CONCLUSION

The optimal operation of the power grid when facing a weather-related event is still a challenge that has attracted many researchers' attention in recent years. This paper studies the potential impacts of heatwaves on power grid operation. Whenever applicable, the network components were modeled by considering the effect of excess temperatures on their operational constraints. The results demonstrated that heatwaves could significantly affect both reserve resources and production cost of the generation and transmission system. One main research direction is to try to understand and model the demand variability during such events with the possibility of increasing the renewable energy capabilities and the impacts on the power grid operation strategy.

REFERENCES

[1] G. A. Meehl, C. Tebaldi, "More intense, more frequent, and longer lasting heat waves in the 21st century", Science 305 (5686) (2004) 994–997..

[2] Executive Office of the President. *Economic Benefits of Increasing Electric Grid Resilience to Weather Outages*; Technical Report; The White House: Washington, DC, USA, 2013.

[3] U.s. energy sector vulnerabilities to climate change and extreme weather, Tech. Rep., U.S. Department of Energy, July 2013. [Online] Available at: https://www.energy.gov/sites/prod/files/2013/07/f2/20130716-EnergySectorVulnerabilitiesReport.pdf.

[4] GAO, Climate change: Energy infrastructure risks and adaptation efforts, 2014. [Online] Available at: https://www.gao.gov/products/GAO-14-74.

[5] F. R. P. Arrieta and E. E. S. Lora, "Influence of ambient temperature on combined-cycle power-plant performance", *Applied Energy*, 80 (2005), pp. 261–272.

[6] J. S. Maulbetsch and M. N. DiFilippo, "Cost and value of water use at combined cycle power plants, California Energy Commission", 2006. [Online] Available at: http://www.energy.ca.gov/2006publications/CEC-500-2006-034/.

[7] X. Ke, D. Wu, J. Rice, M. Kintner-Meyer, and N. Lu, "Quantifying impacts of heat waves on power grid operation", *Applied Energy*, 183 (2016), pp. 504–512.

[8] K. Linnerud, T. K. Mideksa, and G. S. Eskeland, "The impact of climate change on nuclear power supply", *Energy Journal*, 2011, pp. 149–168.

[9] J. Sathaye, L. Dale, P. Larsen, G. Gitts, K. Koy, S. Lewis, and A. Lucena, "Estimating risk to california energy infrastructure from projected climate change", Lawrence Berkeley National Laboratory, (2012). [Online] Available at: http://www.energy.ca.gov/2012publications/CEC-500-2012-057/CEC-500-2012-057.pdf.

[10] L. A. Bollinger and G. P. Dijkema, "Evaluating infrastructure resilience to extreme weather-the case of the dutch electricity transmission network", *European J. Transport & Infrastructure Research*, 16 (2016).

[11] R. Skaggs, *et. al.*, "Climate and energy-water-land system interactions technical report to the us department of energy in support of the national climate assessment", Tech. Rep., Pacific Northwest National Laboratory (PNNL), Richland, WA (US), 2012.

[12] "FAQ: How much electricity is lost in transmission and distribution in the united states?", 2017. [Online] Available at: https://www.eia.gov/tools/faqs/faq.php?id=105&t=3.

[13] R. Jackson, *et.al.*, "Opportunities for energy efficiency improvements in the us electricity transmission and distribution system", ORNL/TM-2015/5. Oak Ridge, TN: Oak Ridge National Laboratory, (2015).

[14] Bador, M., Terray, L., Boé, J., Somot, S., Alias, A., Gibelin, A. and Dubuisson, B., 2017. Future summer mega-heatwave and record-breaking temperatures in a warmer France climate.12(7), p.074025.

[15] Beirlant J, Goegebeur Y, Segers J and Teugels J. 2004. Statistics of extremes: Theory and applications (New York: John Wiley & Sons).

[16] Energy Information Administration, Electric power monthly, [Online] Available at: http://www.eia.gov/electricity/monthly/epm_table_grapher.cfmt=epmt

[17] "1370GQMA Data Sheet", Cummins, [Online] Available at: http://www.cumminspower.com/www/Commercial/SparkIgnited/3266.pdf.

[18] Choobineh, M., Tabares-Velasco, P. C., & Mohagheghi, S. (2016). Optimal energy management of a distribution network during the course of a heat wave. *Electric Power Systems Research, 130, 230–240.*

[19] Y. Riffonneau, S. Bacha, F. Barruel, S. Ploix, "Optimal power flow managementfor grid connected PV systems with batteries," *IEEE Trans. Sustainable Energy* 3(2011 Jul) 309–320.

[20] B. Stone *et al*., "Compound Climate and Infrastructure Events: How Electrical Grid Failure Alters Heat Wave Risk," *Environ. Sci. Technol*., Apr. 2021, doi: 10.1021/acs.est.1c00024.

[21] H. Zhang, G. T. Heydt, V. Vittal, and J. Quintero, "An improved network model for transmission expansion planning considering reactive power and network losses," *IEEE Trans. Power Syst.*, vol. 28, no. 3, pp. 3471–3479, 2013.

[22] P. Dehghanian, Power System Topology Control for Enhanced Resilience of Smart Electricity Grids. PhD thesis, Texas A&M University, 2017